Single and Multi Emitter Terahertz Detectors Using n-Type GaAs/AlGaAs Heterostructures

A. B. Weerasekara, M. B. M. Rinzan, R. C. Jayasinghe, S. G. Matsik, A. G. U. Perera
Dept. of Physics and Astronomy
Georgia State University
Atlanta, GA 30303
e-mail: uperera@gsu.edu

M. Buchanan, H. C. Liu
Institute for Microstructural Sciences
NRC Ottawa, Ont.,
Canada K1A 0R6

G. von Winckel, A. Stintz, S. Krishna
Center for High Technology Materials
University of New Mexico, Albuquerque, NM 87106

***Abstract*— Terahertz detection is demonstrated using $GaAs/Al_xGa_{1-x}As$ n-type heterojunction interfacial work function internal photoemission (HEIWIP) detectors. A smaller workfunction (Δ) needed for terahertz detection can be achieved by using n-doped GaAs emitter and undoped $Al_xGa_{1-x}As$ barrier. A single emitter and a multi emitter n-type $GaAs/Al_xGa_{1-x}As$ HEIWIP detectors were designed, fabricated, and characterized. In both designs, 1×10^{18} cm^{-3} n-type doped GaAs was used as the emitter while $Al_xGa_{1-x}As$ with x = 0.04 for the single emitter detector and x=0.13 for the multi emitter detector was used as the barrier. The threshold frequency of 3.2 THz (93 μm) with peak responsivity of 6.5 A/W at 7.1 THz at 6 K was successfully demonstrated for the single emitter detector while 5 THz (60 μm) threshold frequency and 0.32 A/W peak responsivity was observed for the multi emitter detector at 5 K. In addition, the peak quantum efficiency of ~ 19% and peak detectivity of ~ 5.5×10^{8} Jones under a bias field of 0.7 kV/cm at 6 K were obtained for the single emitter detector.**

I. INTRODUCTION

Terahertz region, which is relatively less explored in the electromagnetic spectrum, lies between 300 GHz and 30 terahertz in the electromagnetic spectrum. In recent years, attention was drawn beyond the infrared region into terahertz region. There is an enormous potential for applications in this spectral range such as medical diagnostic, pharmaceutical, security, wireless communications, and astronomy[1, 2]. However, the main challenge in this field is the lack of suitable terahertz sources and detectors. Thermal detectors that are used in this region are slow in response and are difficult to integrate into focal plane arrays for imaging. Therefore, photon detectors which are faster and easy to integrate into focal plane arrays are good candidates for terahertz applications[3].

In HEIWIP structures, an undoped alloy semiconductor material is used as the barrier and heavily doped semiconductor as the emitter. The internal workfunction, Δ is defined from the top of the Fermi energy level (E_F) in the emitter to the bottom of the conduction band level of the barrier and is given by $\Delta = \Delta_x + \Delta_{narr} - E_F$. Here Δ_x is the conduction band offset between the emitter and the barrier due to Al composition (x), Δ_{narr} is the conduction band narrowing in the emitter layer due to doping, and E_F is the Fremi energy with respect to the bottom of the emitter conduction band. Threshold frequency, f_0 is given by $f_0 = \Delta /4.133$ in terahertz. Here Δ is in meV. The threshold frequency of the detector (f_0) can be tailored by changing the alloy fraction(x)[4, 5].

In general, designing p-type HEIWIP detectors is easier because of the smaller Fermi level shift due to p-doping when compared with n-doping. Therefore, previously reported results on HEIWIP detectors are limited to p-type structures[5-8]. In n-type, the fermi level changes drastically even for smaller change in n-doping due to the smaller effective mass of electron. Because of this, when designing smaller workfunctions (Δ) for terahertz detectors, accuracy of doping should be very precise in order to get results consistent with designs. p-type HEIWIP detectors have shown the ability to push the threshold beyond 5 THz (> 60 μm) limit[4, 6, 9]. Tailorability of threshold frequency f_0 can be achieved by changing Al fractions, and has been demonstrated for p-type HEIWIP terahertz detectors with different Al fractions resulting in f_0 = 4.6, 3.6, and 3.2 THz threshold frequencies[4]. The Al fraction used for the 3.2 THz threshold detector is 0.005 and is close to the practical lower limit for MBE growth. It is not possible to lower the workfunction (Δ) by increasing the emitter doping in p-type HIEWIP since Fermi level will not reach the required level before GaAs becomes metallic as p-doping increases. Therefore, lowering the workfunction (Δ) further may not be possible in p-type HEIWIP devices. If p-doped $Al_xGa_{1-x}As$ is used as the emitters and undoped GaAs as a barrier (inverted structure), workfunction (Δ) can be further reduced by increasing the Al fraction and thereby a lower threshold frequency. However, the reported lowest threshold obtained with inverted structure is 2.3 THz (128 μm). The other alternative is to use n-type GaAs emitters in HEIWIP detectors. For the same Al fraction composition and the same

This work was supported in part by the U. S. NSF under grant No. ECS-0553051.

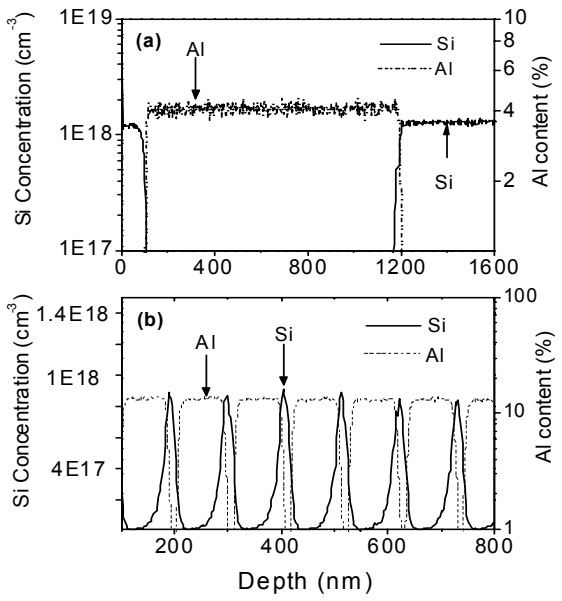

Fig 1: (a) SIMS data of single barrier n-type HEIWIP structure. Top and bottom contact layers (emitters) are n-doped to 1×10^{18} cm^{-3}. Aluminum fraction in the barrier is 4 % (b) SIMS data of the multi emitter structure. Only seven periods are shown for clarity. The aluminum fraction is about 13 % cm^{-3} and Si doping is ~ 1×10^{18} cm^{-3}.

emitter doping concentration, the workfunction in n-type HEIWIP is smaller than that of p-type HEIWIP due to the lower effective mass of electrons compared to the effective mass of holes. According to initial theoretical calculations, it is possible to achieve a threshold frequency below 3 THz in an n-type HEIWIP with a relatively larger Al fraction. For an example, 1 THz threshold frequency can be achievable in n-type HEIWIP with an Al fraction of 0.03 (3.0 %) which is possible in thin film growth techniques. Here, the capability of extending the zero response threshold (f_0) to low terahertz region using n-type emitters in HEIWIP is experimentally demonstrated.

II. Experiment

A. Device Designing

Two HEIWIP (A single emitter and a multi emitter) detector structures were designed to test the performance of n-doped GaAs HEIWIP detectors. The single barrier device structure consists of an undoped 1 μm thick $Al_xGa_{1-x}As$ (x=0.04) barrier layer sandwiched between two n-doped (Si) 1×10^{18} cm^{-3} GaAs contact layers with the top contact being 100 nm and the bottom contact being 700 nm in thickness. GaAs n-doped to 5×10^{18} cm^{-3} with Si was used as the substrate to enhance the light reflection from the substrate. The top and the bottom contact layers work as emitters for reverse and forward bias operations. The Si doping concentration and the Al fraction were verified by secondary ion mass spectrometry (SIMS) as shown in Fig. 1 (a). The thickness of the top contact layer was kept to 100 nm to allow a substantial amount of light to pass through to the bottom contact. The multi emitter device consists of twelve periods of 1×10^{18} cm^{-3} n-doped 20 nm thick GaAs emitter and undoped 80 nm thick $Al_{0.13}Ga_{0.87}As$ barrier. The top and bottom contact layers were 1×10^{18} cm^{-3} n-doped with 100 and 700 nm thicknesses respectively and 5×10^{18} cm^{-3} n-doped GaAs was used as the substrate. NiGeAu was deposited on the bottom and the top layers as ring ohmic contacts to make electrical contacts. Note that the highly doped substrate is electrically isolated from the active layers.

B. Device Characterization

1) Single Emiter device

The electron gas in the single emitter structure should be treated as a 3D distribution. The calculated Fermi energy in the emitter layers of the single barrier device, E_F is 55 meV while the conduction band discontinuity in the GaAs/AlGaAs interface is 32 meV for x = 0.04. Considering band gap narrowing [10] of 35 - 45 meV in the GaAs emitter layer due to 1×10^{-18} cm^{-3} n - doping, the calculated workfunction (Δ) of the single barrier device is between ~ 10 -20 meV, which corresponds to 2.4 - 5.0 THz (125 -60 μm) cutoff frequency. Dark current-voltage measurements were performed on the devices from 4.2 to 120 K to obtain workfunction (Δ) using Arrhenius analysis. According the estimated workfunction using Arrhenius analysis is 13 - 14 meV (88 – 95 μm) for the single emitter device. Spectral measurements at 6 K were performed using a fast fourier transform infrared spectrometer (FTIR) and a silicon composite bolometer was used to calibrate the raw

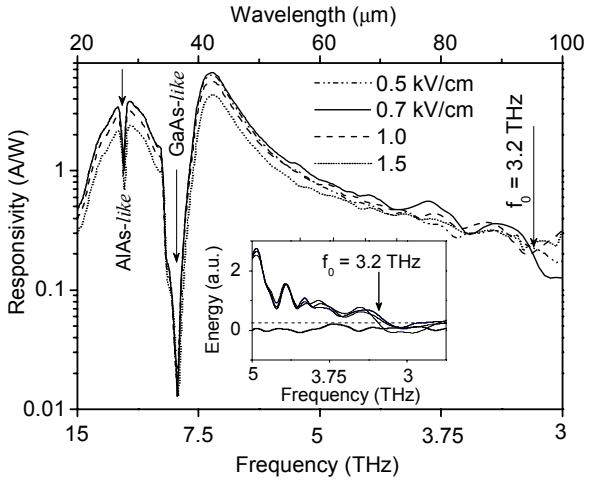

Fig 2: Spectral response for single emitter device at 6 K. The threshold frequency of 3.2 THz (93 μm) was determined by considering the instrument noise level as shown in the inset. The peak response was found to be 6.5 A/W at 7.1 THz. Two narrow dips are due to the GaAs and AlAs like phonons.

spectra. The measured spectral responses for different bias fields are shown in Fig. 2. The zero response threshold frequency, which is found to be 3.2 THz (93 μm), was estimated by considering instrument noise level. The maximum peak response of 6.5 A/W at 7.1 THz (42 μm) was obtained at 0.7 kV/cm bias field. A strong light reflection occurs around 11 THz (27 μm) and 8.3 THz (36 μm) due to the AlAs-*like* and GaAs optical phonons, giving two minima around 11 THz (27 μm) and 8.3 Thz (36 μm) in the responsivity spectra. Up to now, the lowest threshold frequency reported for HEIWIP detectors is 2.3 THz (128 μm)[6]. It is noteworthy that the response of the single barrier detector reported here matches the 10 emitter p-type detector reported in ref.[6]. The peak values of responsivity (R_P), quantum efficiency (η_p), and detectivity (D_p^*) at 7.1 THz for different bias fields are given in Table I. The detectivity was calculated using the shot noise. The device response decreases with temperature and vanishes after 25 K. The device can also be operated under reverse bias and R_p of 1.7, 1.1, and 0.7 A/W at 10 THz (30 μm) were observed at -0.25, -0.5, and -0.75 kV/cm bias respectively.

TABLE I.

The peak responsivity (Rpeak), peak quantum efficiency (η), and detectivity (D*) are given at different applied bias fields for the single emitter detector.

Bias Field (kV/cm)	R_{peak} (A/W)	η (%)	D^* (Jones)
0.2	3.0	8.9	5.5
0.5	6.1	18.2	6.4
0.7	6.5	18.9	5.5
1.0	5.5	16.5	3.4
1.5	4.1	12.3	2.1

2) Multi Emitter Device

Spectral response measurements were carried out for the multi layer device as in the single emitter device case. The calculated workfucntion (Δ) for the multi emitter device must be larger than 60 meV which corresponds to a threshold shorter than 20 μm. However, a workfunction (Δ) of ~ 22 meV (~ 5 THz) was obtained from Arrhenius analysis. The threshold frequency obtained from the spectral measurements is ~ 5 THz (20 meV) as shown in Fig. 3 and is in close agreement with the arrhenius analysis. According to the SIMS measurements, a considerable amount of doping migration into the barrier layer is visible. This doping migration can change the Fermi level alignment from the expected situation across the interface causing the effective barrier height much smaller. It should be mentioned that further studies are needed to understand how this discrepancy occurs in the multilayer detector. Furthermore, the spectral responsivity of the multi emitter detector is lower than the single emitter device and can be

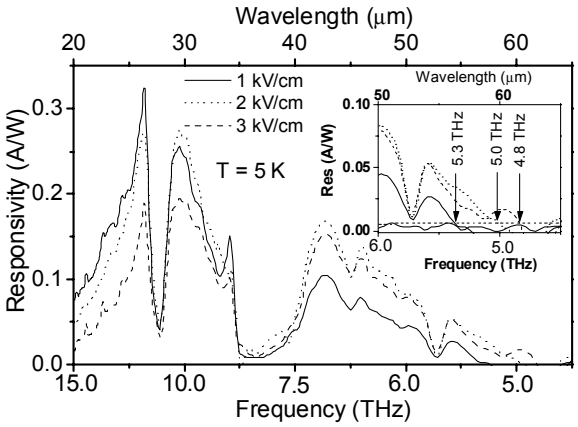

Fig 3: The responsivity of multi emitter device with three different applied bias fields at 5 K. The maximum responsivity of 0.32 A/W at 11 THz at the bias filed of 1 kV/cm is obtained. Threshold frequencies of 5.3, 5.0, and
4.8 THz were estimated for bias fields of 1.0, 2.0, and 3.0 kV/cm respectively using the system noise level (see the inset)

attributed to the doping migration in the multi emitter device. Due to the doping migration, density of states can be less leading to low photoabsorption efficiency.

III. PHOTORESPONSE MODELING

Spectral responsivity for HEIWIP detectors can be carried out as discussed in Ref.[5,11]. The photo responsivity R can be given as in Eq. [1].

$$R(\lambda) = \frac{q\eta\lambda}{hc} \quad \text{..... [1]}$$

Where, q is the electron charge, η is the total quantum efficiency, h is the Plank constant, and c is the speed of light. Total quantum efficiency depends on the light absorption efficiency in the emitter layer (η_a), photoexcited carrier emission efficiency (η_e) over the workfunction (Δ), and the carrier collection efficiency (η_c.) which can be considered as unity in most cases. The absorption efficiency (η_a) can be calculated using the free carrier absorption mechanism[5]. Photoexcited carrier emission efficiency ((η_e) can be calculated using the escape cone model [11, 12] with or without considering phonon emission. The spectral response including phonon emission was modeled for the single emitter device and is shown in Fig. 4. Model calculation matches well in the lower frequency range (< 10 THz). There is a small discrepancy between the calculated and the experimental spectra above 11 THz. This discrepancy may be due to energy independent scattering length assumption.

IV. DISCUSSION AND CONCLUSION

In this work, n-type GaAs/AlGaAs HEIWIP terahertz detectors have been successfully demonstrated. When compared with p-type HEIWIP detectors, a smaller threshold frequency can be obtained with a relatively higher Al

fraction. Thereby, n-type HEIWIP devices are favorable for terahertz detection. An Al fraction of 0.005, which is around the lowest limit for MBE, was used to obtain 3.2 THz threshold in a p-type HEIWIP detector[4] while the same threshold frequency can be obtained with Al fraction of 0.04 in the n-type HEIWIP detector as shown in this study. Ability to design smaller workfunction with higher Al fractions in n-type GaAs is favorable for growth. Extending the threshold frequency below 3 THz in photon detectors is possible. In addition, successful modeling for n-type GaAs/AlGaAs HEIWIP devices was also carried out.

REFERENCES

[1] P. H. Siegel, "Terahertz Technology," *IEEE Transaction on Microwave Theory and Techniques* ol. 50, pp. 910-928, 2002.

[2] P. H. Siegel, "Terahertz technology in biology and medicine," *Microwave Theory and Techniques, IEEE Transactions on*, vol. 52, pp. 2438-2447, 2004.

[3] A. Rogalski, "Infrared detectors: status and trends," *Progress in Quantum Electronics*, vol. 27, pp. 59-210, 2003.

[4] S. G. Matsik, M. B. M. Rinzan, A. G. U. Perera, H. C. Liu, Z. R. Wasilewski, and M. Buchanan, "Cutoff tailorability of heterojunction terahertz detectors," *Appl. Phys. Lett.*, vol. 82, pp. 139-141, 2003.

[5] D. G. Esaev, M. B. M. Rinzan, S. G. Matsik, and A. G. U. Perera, "Design and optimization of GaAs/AlGaAs heterojunction infrared detectors," *J. Appl. Phys.*, vol. 96, pp. 4588-4597, 2004.

[6] M. B. M. Rinzan, A. G. U. Perera, S. G. Matsik, H. C. Liu, Z. R. Wasilewski, and M. Buchanan, "AlGaAs emitter/GaAs barrier terahertz detector with a 2.3 THz threshold," *Appl. Phys. Lett.*, vol. 86, pp. 071112, 2005.

[7] S. G. Matsik, M. B. M. Rinzan, D. G. Esaev, A. G. U. Perera, H. C. Liu, and M. Buchanan, "20 μm cutoff heterojunction interfacial work function internal photoemission detectors," *Appl. Phys. Lett.*, vol. 84, pp. 3435-3437, 2004.

[8] D. G. Esaev, S. G. Matsik, M. B. M. Rinzan, A. G. U. Perera, H. C. Liu, Z. R. Wasilewski, and M. Buchanan, "Resonant Cavity Enhanced GaAs/AlGaAs IR Detectors," *SPIE Proc.*, vol. 4999, pp. 467-477, 2003.

[9] A. G. U. Perera, S. G. Matsik, M. B. M. Rinzan, A. Weerasekara, M. Alevli, H. C. Liu, M. Buchanan, B. Zvonkov, and V. Gavrilenko, "The Effects of Light-Heavy Hole Transitions on the Cutoff Wavelengths of Far Infrared Detectors," *Infrared Phys. and Tech.*, vol. 44, pp. 347-353, 2003.

[10] H. Yao and A. Compaan, "Plasmons, photoluminescence, and band-gap narrowing in very heavily doped n-GaAs," *Applied Physics Letters*, vol. 57, pp. 147-149, 1990.

[11] A. G. U. Perera, H. X. Yuan, and M. H. Francombe, "Homojunction internal photoemission far-infrared detectors: Photoresponse performance analysis," *J. Appl. Phys.*, vol. 77, pp. 915-924, 1995.

[12] J. M. Mooney and J. Silverman, "The theory of hot-electron photoemission in Schottky-barrier IR detectors," *IEEE Trans. Electron Devices*, vol. 32, pp. 33-39, 1985.